Available online at www.sciencedirect.com
SCIENCE DIRECT
Polymer 47 (2006) 2548–2554
polymer
www.elsevier.com/locate/polymer

The unfolding and folding dynamics of TNfnALL probed by single molecule force–ramp spectroscopy

Meijia Wang, Yi Cao, Hongbin Li *

Department of Chemistry, The University of British Columbia, Vancouver, BC, Canada V6T 1Z1

Received 15 November 2005; received in revised form 1 December 2005; accepted 3 December 2005
Available online 7 February 2006

Abstract

Tenascin, an important extracellular matrix protein, is subject to stretching force under physiological conditions and plays important roles in regulating the cell–matrix interactions. Using the recently developed single molecule force–ramp spectroscopy, we investigated the unfolding–folding kinetics of a recombinant tenascin fragment TNfnALL. Our results showed that all the 15 FnIII domains in TNfnALL have similar spontaneous unfolding rate constant at zero force, but show great difference in their folding rate constants. Our results demonstrated that single molecule force–ramp spectroscopy is a powerful tool for accurate determination of the kinetic parameters that characterize the unfolding and folding reactions. We anticipate that single molecule force–ramp spectroscopy will become a versatile addition to the single molecule manipulation tool box and greatly expand the scope of single molecule force spectroscopy.

1. Introduction

Over the last decade, single molecule atomic force microscopy (AFM) has evolved into a powerful experimental tool to investigate the nanomechanical properties and force-induced conformational changes for a wide range of polymers, ranging from synthetic polymers to DNA and proteins [1–3]. In particular, single molecule AFM has become a unique technique to probe the folding and unfolding dynamics at the single molecule level [1,4–12]. When stretched by a mechanical force, proteins will undergo force-induced unfolding reactions along the reaction coordinate that is predefined by the force vector acting on the proteins, providing a novel approach to investigate the complex energy landscape of protein folding and unfolding [13–21]. In addition, single molecule AFM also mimics the natural settings for mechanical proteins in vivo, which are subject to mechanical stretching forces under physiological conditions, and promises to provide information that is physiologically more relevant [22–27]. Therefore, single molecule AFM has been widely used to probe the mechanical properties of naturally occurring mechanical proteins and has provided tremendous insight into the underlying molecular mechanisms. These developments have resulted in a new emerging field: protein mechanics [28].

The most widely used mode of single molecule AFM is the constant velocity mode. In this mode, a modular protein is stretched between the AFM tip and the solid substrate at a constant velocity (Fig. 1). The stretching force triggers the mechanical unfolding of the individual domains and generates force–extension curves with the characteristic saw-tooth pattern appearance. Each individual saw-tooth peak corresponds to the mechanical unfolding of the individual domain [13,15,29]. In a constant velocity AFM stretching experiment, the extension is the independent variable and the restoring force generated by a protein changes in a complex non-linear fashion as a function of the extension. The nonlinearity of the force–extension relationship originates from the non–linear nature of the entropic elasticity of a polymer chain [30]. During the force–extension measurements, the restoring force on the protein changes as a result of the domain unfolding and the resultant increment of the contour length of the protein molecule, creating the complex saw-tooth patterns. The unfolding force of a protein in constant velocity experiments depends on two factors, the number of domains remaining folded and the progressively increasing compliance of the protein chain. These two factors compete with each other and cause the mechanical unfolding of individual domains to be history dependent [31] in a constant velocity experiment. This is often called 'N-effect'. The complex elastic behavior has made it difficult to derive an analytic solution to describe the mechanical unfolding of proteins and allow for the

* Corresponding author.
E-mail address: hongbin@chem.ubc.ca (H. Li).

0032-3861/$ - see front matter © 2006 Elsevier Ltd. All rights reserved.
doi:10.1016/j.polymer.2005.12.086

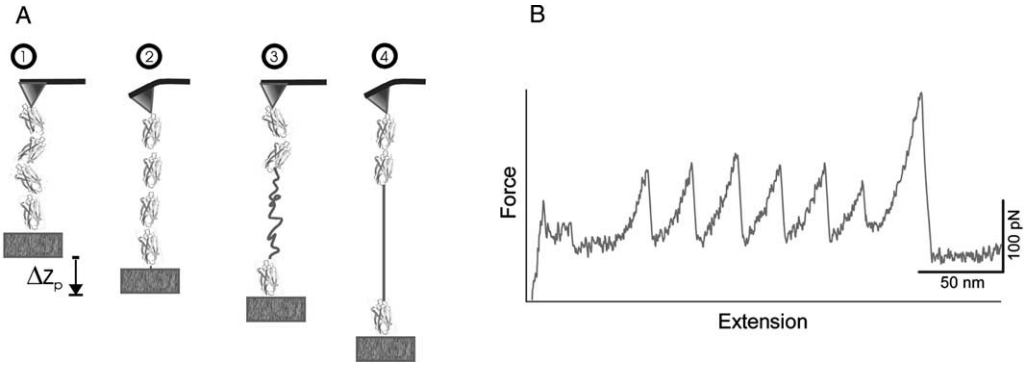

Fig. 1. The mechanical unfolding of tandem modular protein in the constant velocity mode of AFM. (A) shows the schematic of the AFM experiment. In this mode, the protein is pulled at a constant velocity. The unfolding of the individual domains results in force–extension curves of the characteristic saw-tooth pattern (B), in which the saw-tooth peak corresponds to the sequential mechanical unfolding of individual domain.

direct determination of the kinetic parameters, such as the unfolding rate constant at zero force, that characterize the mechanical unfolding reaction of a protein. Currently, these parameters are obtained through either Monte Carlo simulations or numerical fitting [15,23,32,33].

Recently, it has become possible to unfold a protein under a predefined constant force, leading to the so-called force-clamp spectroscopy [34–36]. In this mode of operation, a protein can be stretched at a constant force by AFM via a force-feedback system. The stretching force can be set as any arbitrary waveform. If the stretching force increases in a linear ramp, it will give rise to the so-called force–ramp spectroscopy. In this mode, a modular protein is stretched by a linear ramp of stretching force. Compared with the constant velocity mode of AFM, force–ramp mode of AFM sets the force directly and the extension changes as a function of the force. In this mode of operation, the mechanical unfolding of tandem modular protein will result in the stepwise elongation of the protein, giving rise to the staircase appearance of the exetension–force curve [34]. The probability density function of the unfolding forces can be solved analytically, promising a more accurate measurement for the kinetic parameters [34,35].

In this paper, we will utilize the force–ramp spectroscopy to study the mechanical unfolding kinetics of a recombinant human tenascin-C fragment TNfnALL, which is composed of all the 15 fibronectin type III domains (FnIII) of tenascin [37]. Tenascin is an extracellular matrix protein conserved in all vertebrates [38]. Tenascin plays important roles in regulating the interactions between the cell and the extracellular matrix [39–41]. Tenascin-C is mostly expressed in tissues that are subject to heavy tensile load, such as the myotendonious junction, and is believed to provide elasticity and mechanical strength [42,43]. Under physiological conditions, tenascin-C is subject to mechanical stretching force. Using force-spectroscopy techniques to probe the unfolding and folding dynamics promises to provide information that is physiologically more relevant. Previous AFM studies demonstrated that tenascin can extend to several times its resting length via force-induced unfolding of the FnIII domains [24,37,44]. In this paper, we will use force–ramp spectroscopy to investigate the unfolding kinetics of TNfnALL, and compare the results with those obtained from constant velocity experiments. In addition, we will also expand the scope of force–ramp spectroscopy to enable the study of the folding dynamics of individual TNfnALL molecules.

2. Materials and methods

2.1. Materials

TNfnALL, composed of 15 FnIII domains of human tenascin-C, is a generous gift from Harold Erickson. TNfnALL was dissolved in PBS buffer at a concentration of 400 μg/mL.

2.2. Single molecule force–ramp spectroscopy

Single molecule force–ramp spectroscopy studies were carried out on a custom built AFM setup, which is similar to that reported in Ref. [36]. Si_3N_4 cantilevers with a typical spring constant of 40 pN/nm (Veeco, Santa Barbara, CA) were used in our experiments. The individual AFM cantilever was calibrated before and after each AFM experiment using thermal equipartition theorem [45,46]. In a typical force–ramp experiment, 2 μL TNfnALL sample was deposited onto a clean glass coverslip which was covered by ~50 μl PBS, and allowed for adsorption for 10 min. During an AFM experiment, the AFM tip was brought into contact with the protein sample for 2 s at a contact force of ~200 pN. Due to non-specific interaction, TNfnALL can adsorb onto the AFM tip, allowing itself to be stretched between the AFM tip and the solid substrate. Then TNfnALL was subject to a stretching force which increases linearly from zero to the maximum setting force as a function of time. The ramp rate varies from 20 to 1000 pN/s. Unfolding events that are 5 ms apart in time can be readily resolved in our force–ramp spectroscopy experiments.

3. Results and discussion

3.1. The mechanical unfolding of TNfnALL under force–ramp spectroscopy

In a force–ramp experiment, TNfnALL is stretched with a mechanical force that increases linearly as a function of time

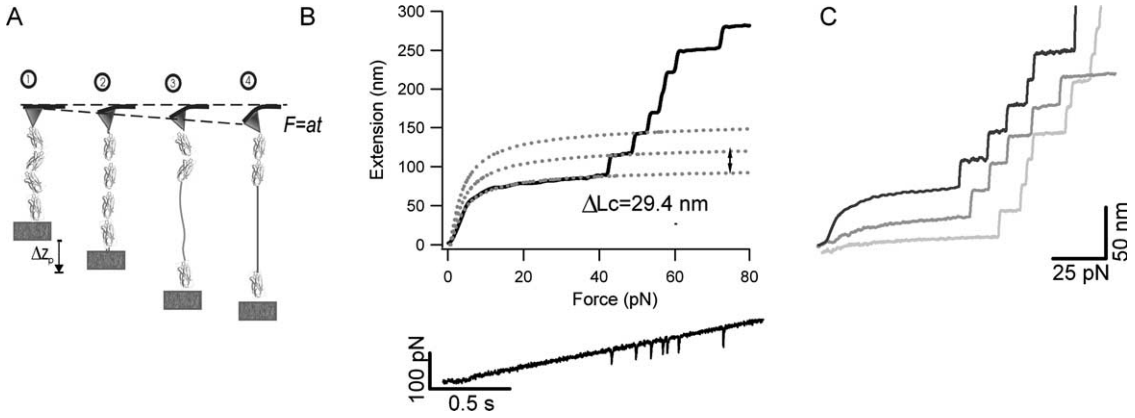

Fig. 2. The mechanical unfolding of single TNfnAll molecules measured by the force–ramp mode of AFM. (A) A schematic of single molecule force ramp spectroscopy. In this mode, the stretching force F increases in a linear fashion $F=at$ (where a is the ramp rate and t is the time), and the end-to-end distance of a single tandem modular protein is measured as a function of F. The mechanical unfolding of individual domains gives rise to the staircase appearance of the resulting extension–force curves, as shown in (B) and (C). (B) A typical extension–force curve measured in force–ramp spectroscopy experiments. The extension–force curve (upper panel) is characterized by the step-wise elongation of the end-to-end distance and can be well described by the worm-like-chain model of polymer elasticity (dotted lines). WLC fits measures a contour length increment of ~29 nm for FnIII domains upon their mechanical unraveling. The measured force signal (lower panel) as a function of time is shown at the bottom. Due to the limited frequency response, transient relaxation of the force correlates with the domain unfolding event and is shown as spikes. (C). Typical recordings of length vs. time for single TNfnALL protein stretched with a linearly increasing force (the ramp rate is 100 pN/s).

(Fig. 2A). Stretching single TNfnALL molecules with a force–ramp generates exetension–force curves of the characteristic staircases appearance [34], as those shown in Fig. 2(B and C). Preceding the staircases, the exetension–force curves showed an initial fast, non-linear elongation of the protein at low forces (Fig. 2B, upper panel), which can be well described by the worm-like-chain model of polymer elasticity [30]. The individual steps are resulted from the sequential mechanical unfolding of the FnIII domains in TNfnALL. In force-time trace (Fig. 2B, lower panel), we observed a series of spikes, during which the force transiently relaxed to a lower value. The occurrence of the 'spikes' correlates well with the stepwise elongation of the proteins and is due to the finite frequency response of our analogue force-feedback electronics (which is typically 3–5 ms in our current setup). This unintended feature allows us to resolve the mechanical unfolding events directly from the force-time traces.

The unfolding staircases occurred at different forces and are of similar amplitudes (Fig. 2B and C). The histogram of the step sizes (Fig. 3) shows a narrow distribution with an average step size of 25.0±0.9 nm (Gaussian fit, average±SD). WLC fits to the experimental data indicate that a step size of 25 nm corresponds to a contour length increment of ~29 nm upon domain unfolding (Fig. 2B). Tenascin FnIII domains contain 90 amino acids on average (between 89 and 92 amino acids). The contour length of a fully extended FnIII domain measures 90×0.36=32.4 nm. The distance between the N- and C-termini in a folded FnIII domain is about 3.6 nm (measured from the crystal structure of the third FnIII domain) [47]. Hence the mechanical unfolding of an FnIII domain will lengthen the protein by 28.8 nm, in agreement with our experimental results. The measured contour length increment indicated that the mechanical unfolding of FnIII domains corresponds to an all-or-none process and no intermediate state is present along the mechanical unfolding pathway. Therefore, the mechanical unfolding of FnIII domains can be treated as a simple two-state process.

A histogram of the unfolding forces at which unfolding events occurred is plotted in Fig. 4. At a force ramp rate of 100 pN/s, we observed that the mechanical unfolding of FnIII domains can occur at forces ranging from 30 to 150 pN. In addition, the distribution of the unfolding forces appears to be asymmetric and peaks at around 100 pN.

3.2. Two-state unfolding and analytical treatment of unfolding

Based on a two-state model, Evans' group and Schulen's group studied the unbinding of a ligand–receptor pair under a linearly increasing mechanical stretching force, and derived the probability and probability density functions for the unbinding forces [48,49]. As the unfolding of FnIII domains is a simple

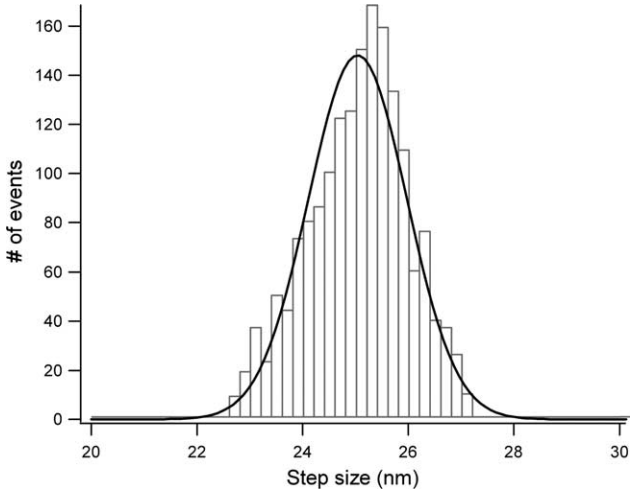

Fig. 3. The histogram of the step sizes upon the mechanical unfolding of FnIII domains. A Gaussian fit (solid line) to the experimental data measures an average step-size of 25.0±0.9 nm (average±SD).

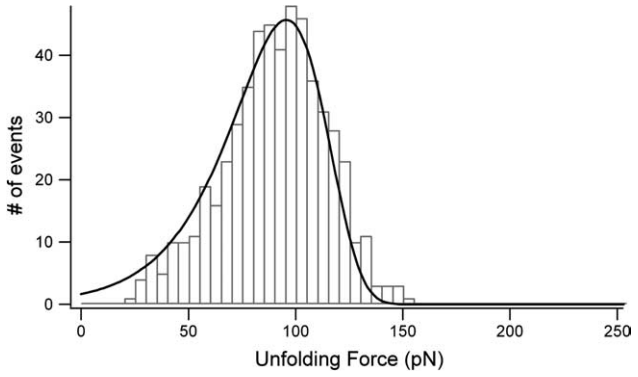

Fig. 4. The distribution of unfolding probability density for FnIII domains. Grey bars correspond to the unfolding force histogram measured for FnIII domains at a force–ramp rate of 100 pN/s ($n=544$). A least square fit (solid line) of Eq. (2) to the experimental data results in an excellent fit with $\alpha_0 = 0.06\ s^{-1}$ and $\Delta x_u = 0.19$ nm.

two-state process, it is possible to directly apply these derivations to the analysis of the mechanical unfolding of FnIII domains. The unfolding rate constant ($\alpha(F)$) depends upon the stretching force F, $\alpha(F)=\alpha_0 \exp(F\Delta x/k_BT)$, where α_0 is the unfolding rate constant at zero force, and Δx is the unfolding distance between the folded state and the transition state, k_B is the Boltzmann constant, T is the absolute temperature [50]. The probability of unfolding can be written as: $dP_u=(1-P_u)\alpha(t)dt$, where $\alpha(t)$ is the unfolding rate constant at time t. The stretching force acting on the protein is related to the time by the force–ramp rate, $F=at$, where a is the force–ramp rate. Solving the differential equation gives the probability distribution of unfolding as a function of the stretching force:

$$P_u(F) = 1 - e^{-\frac{\alpha_0 k_B T}{a\Delta x}\left(e^{\frac{F\Delta x}{k_B T}}-1\right)} \quad (1)$$

This equation predicts a sigmoid relationship between the unfolding probability and the stretching force. By taking the derivative of the unfolding probability, we can obtain the unfolding probability density as a function of the stretching force. The unfolding probability density describes the predicted shape of the unfolding force histogram at a given ramp rate.

$$\frac{dP_u}{dF} = \frac{\alpha_0}{a} e^{\frac{F\Delta x}{k_B T}} e^{-\frac{\alpha_0 k_B T}{a\Delta x}\left(e^{\frac{F\Delta x}{k_B T}}-1\right)} \quad (2)$$

Although this derivation is based upon the unfolding of a single protein domain, the results can be directly applied to the force–ramp spectroscopy experiments on polyproteins [34,35]. In force–ramp spectroscopy experiments, the force is an independent variable and all of the domains are subject to the same force at the same time. Under this experimental setting, one force–ramp experiment of a polyprotein of N domains is equivalent to carrying out force–ramp experiment on a single domain independently for N times. The so-called 'N-effect', encountered in force–extension experiments, no longer exists in force–ramp experiments. Therefore, Eqs. (1) and (2) represent exact analytic solutions to the force–ramp experiments. In addition, utilizing polyproteins in force–ramp experiments also greatly improves the experimental throughput and statistics.

Hence, we now use Eq. (2) to fit the unfolding force distribution (Fig. 4) obtained from force–ramp spectroscopy experiments on TNfnALL at a ramp rate of 100 pN/s. A non–linear least square fit to the experimental data produces an excellent fit with parameters of $\alpha_0 = 0.06\ s^{-1}$, $\Delta x_u = 0.19$ nm (Fig. 4, solid line). Both the peak value and the width of unfolding force histogram are important. The width of the unfolding force histogram is directly related to the unfolding distance Δx_u, while the peak unfolding force is a product of the unfolding rate constant α_0 and Δx_u. A force–ramp experiment at one ramp speed is in principle sufficient to recover both α_0 and Δx_u.

3.3. The most probable unfolding force depends upon the ramp rate

The most probable unfolding force at a given ramp rate can also be determined by taking the derivative of Eq. (2) with respect to F to zero, as shown in Eq. (3)

$$F^* = \frac{k_B T}{\Delta x}\left[\ln a + \ln\left(\frac{\Delta x}{\alpha_0 k_B T}\right)\right] \quad (3)$$

where F^* is the most probable unfolding force, which is linearly dependent upon ln (ramp rate). From a semi-log plot of the unfolding force vs ramp rate, the spontaneous unfolding rate constant and the distance between the native state and the transition state can be readily determined from the slope and the intercept at the x-axis. The experimental results are shown in Fig. 5. A linear fit of Eq. (3) to the experimental data predicts a spontaneous unfolding rate constant of $0.099\ s^{-1}$ and an unfolding distance of Δx_u of 0.2 nm (correlation coefficient 92.4%), which are in close agreement with the fit from Eq. (2).

It is also evident that, although 15 FnIII domains in TNfnALL are different in their primary sequences, it is sufficient to use one set of kinetic parameters to describe their unfolding reactions. This result indicates

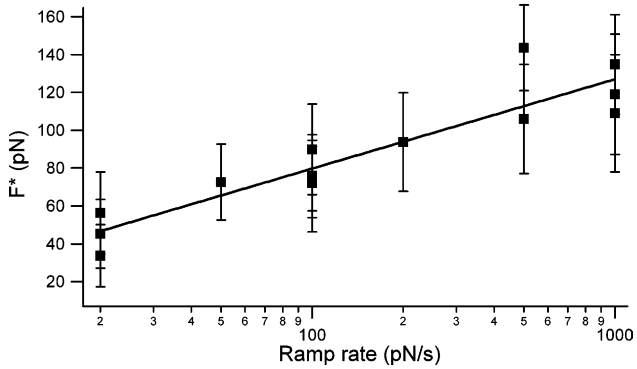

Fig. 5. The ramp-rate dependence of the most probable unfolding forces F^* for TNfnALL. The peak value of the Gaussian fit to the unfolding force histogram was taken as F^*. Symbols correspond to F^* measured from three independent experiments. A fit of Eq. (3) to the experimental data gave $\alpha_0 = 0.099\ s^{-1}$, and $\Delta x = 0.20$ nm.

that all the 15 FnIII domains have similar spontaneous mechanical unfolding rate constant at zero force, similar to the observation from previous constant velocity measurements [24,44].

It is of importance to note that the unfolding rate constant obtained using force–ramp spectroscopy is significantly larger than those obtained from early constant velocity experiments ($0.06\,s^{-1}$ vs $4.6\times10^{-4}\,s^{-1}$ and $3\times10^{-5}\,s^{-1}$) [24,44] and our own measurements (unpublished result). The unfolding distance is also smaller than that estimated in constant velocity experiments. This big contrast between the constant velocity and force–ramp spectroscopy was also evident in the force spectroscopy studies on a small protein ubiquitin [18,35]. Certain experimental issues are likely to contribute partially to this discrepancy. During a force–ramp experiment, a polyprotein can detach from the AFM tip or substrate before all of its FnIII domains unfold. Hence it is possible that exetension–force curves measured in force–ramp experiments contain fewer unfolding events than one should have observed if all the domains in the polyprotein chain were to unfold. This will result in overcounting the unfolding events occurring at lower forces and thus skew the unfolding probability distribution function towards lower force. Certainly, this possible pitfall will result in overestimation of the unfolding rate constant. However, this overestimation cannot fully account for the discrepancy. Since Eqs. (2–4) are formulated specifically for the force–ramp experiments, it is possible that force–ramp experiments may produce estimations of the kinetic parameters that are more likely to represent the true kinetic signature of proteins. Further work is needed to investigate this point more thoroughly.

3.4. Refolding experiments using force–ramp spectroscopy

It has been demonstrated in constant velocity measurements that it is possible to repeatedly stretch and relax the same protein for many cycles to allow the protein to undergo repeated unfolding and refolding reactions [13,15]. Here, we demonstrate that it is possible to directly measure the folding kinetics of a single protein using force–ramp spectroscopy. Compared with the constant velocity folding experiments, refolding studies using force–ramp approach allows one to carry out refolding experiments at well–defined forces, promising a more accurate determination of the folding rate constant and folding distance.

During a force–ramp experiment, it is possible to repeatedly stretch and relax the same protein if we limit the pulling force such that the protein will not detach from the AFM tip or substrate. Using a double pulse protocol (Fig. 6A), we measured the folding kinetics of single TNfnALL molecules. In the first force–ramp pulse, the protein is stretched by a force–ramp and the FnIII domains unfold sequentially one-by-one, giving rise to the well-resolved extension steps. In the first unfolding trace shown in Fig. 6A, four unfolding events were observed, indicating that a stretch of four FnIII domains were pulled and unfolded in the molecule being stretched. When the force reached the maximum setting-force, the protein is rapidly relaxed to zero force (typically within 2 ms). Then the protein is allowed to refold at zero force for a fixed period of time of 50 ms, and then stretched again by the second pulse of force–ramp. During the second pulse, one unfolding step was observed, indicating that only one of the four domains refolded during the 50 ms waiting period. By varying the waiting period at zero force, we have now measured the folding kinetics of FnIII domains (Fig. 6B). In contrast to the

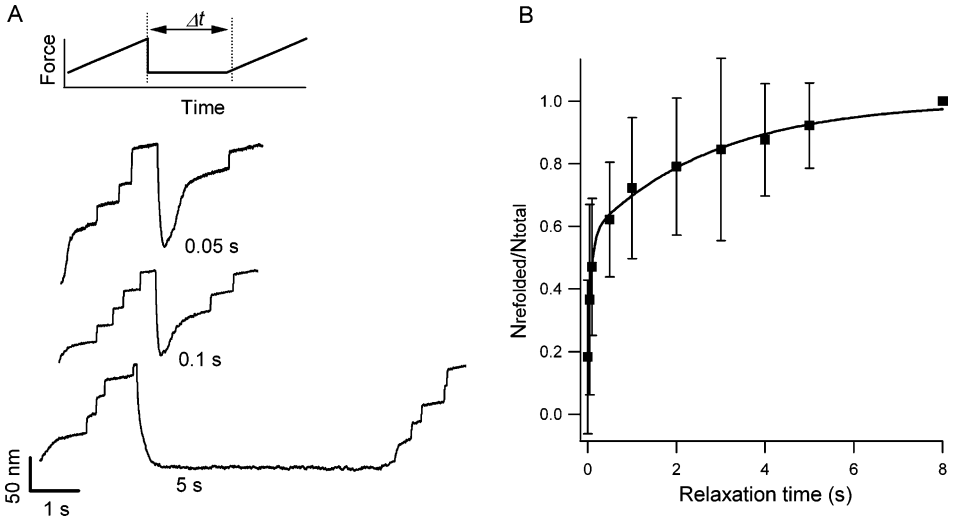

Fig. 6. Refolding kinetics of a single TNfnALL protein measured by force–ramp spectroscopy. (A) A double-pulse protocol was used to allow a single TNfnALL molecule to undergo repeated unfolding and refolding cycles. A single TNfnALL protein was stretched and unfolded in the first force–ramp pulse to identify the total number of domains (N_{total}) in the chain. After complete unfolding of all the FnIII domains, the unfolded chain was relaxed to zero force within 2 ms. The unfolded protein was allowed to refold at zero force for Δt. The protein was then stretched and unfolded by the second pulse, which measures the number of domains ($N_{refolded}$) that have refolded. Three representative refolding traces are shown. (B) Plot of $N_{refolded}/N_{total}$ vs Δt. Each symbol shown here is the average of (from left to right) 38, 24, 25, 19, 20, 19, 18, 18, 18, 15 data points obtained from three independent experiments. The folding kinetics can be fitted with a double-exponential function: $N_{refold}/N_{total} = A(1-e^{-\beta_1 t}) + (1-A)(1-e^{-\beta_2 t})$, which gave $A=0.55$, $\beta_1=19.9\,s^{-1}$, $\beta_2=0.37\,s^{-1}$.

single exponential two-state folding kinetics observed on small proteins [15,22,51] using single molecule AFM, the folding kinetics of TNfnALL contains at least two exponential components. We have fitted the folding kinetics using a double exponential function:

$$\frac{N_{\text{refold}}}{N_{\text{total}}} = A(1-e^{-\beta_1 t}) + (1-A)(1-e^{-\beta_2 t})$$

where $N_{\text{refold}}/N_{\text{total}}$ represents the fraction of folded FnIII domains, and β_1 and β_2 correspond to the rate constant. We found that the faster folding rate constant is 19.9 s^{-1} and the slower one is 0.4 s^{-1}. TNfnALL contains 15 different FnIII domains, hence the folding kinetics measured here is a convoluted average behavior of different FnIII domains. It is likely that this multiple-exponential folding kinetics of TNfnALL is due to the heterogeneity of the folding rate constants among different FnIII domains in TNfnALL. This conclusion is in accordance with the chemical folding studies of tenascin FnIII domains [52] and is also supported by our recent measurements on the folding kinetics of a polyprotein made of eight identical tandem repeats of the third FnIII domain, which shows a simple two-state folding kinetics with a rate constant of 1.2 s^{-1} (unpublished results). Based on these results, we can now separate the FnIII domains into two groups: one group folds at an average rate constant of 19.9 s^{-1}, and a second group folds much slower with an average rate constant of 0.4 s^{-1}. The diversity of the folding rate constants among different FnIII domains is in sharp contrast to the homogeneity of their unfolding rate constants. It has been shown that tenascin FnIII domains can undergo domain swapping, resulting in misfolded FnIII domains [53]. Previous single molecule AFM studies on immunoglobulin domains of titin showed that, arranging Ig domains with different folding rate constant in tandem effectively minimizes the probability of misfolding between different Ig domains [53]. Similar to titin, it is likely that the vastly different folding rate constants among different FnIII domains may also serve as a mechanism to minimize the chances for FnIII domains to misfold.

4. Conclusion

In summary, we have investigated the folding and unfolding dynamics of FnIII domains in tenascin using single molecule force–ramp spectroscopy. Our results elaborate that single molecule force–ramp spectroscopy is a powerful tool allowing for the accurate determination of the kinetic parameters, such as unfolding rate constant and unfolding distance. We also demonstrate that it is possible to repeatedly stretch and relax the same molecule to measure its folding kinetics using force–ramp spectroscopy. Our results revealed that all the 15 FnIII domains of TNfnALL share similar spontaneous unfolding rate constant at zero force and similar unfolding distance, but have very different folding rate constants. This feature may have important implications in preventing misfolding event for tenascin molecules under physiological conditions.

Acknowledgements

This work is supported by National Sciences and Engineering Research Council of Canada (NSERC), Canadian Foundation for Innovation (CFI), Canada Research Chair Program and the University of British Columbia.

References

[1] Clausen-Schaumann H, Seitz M, Krautbauer R, Gaub HE. Curr Opin Chem Biol 2000;4(5):524–30.
[2] Janshoff A, Neitzert M, Oberdorfer Y, Fuchs H. Angew Chem Int Ed 2000;39(18):3213–37.
[3] Zhang W, Zhang X. Prog Polym Sci 2003;28(8):1271–95.
[4] Zhuang X, Rief M. Curr Opin Struct Biol 2003;13(1):88–97.
[5] Carrion-Vazquez M, Oberhauser AF, Fisher TE, Marszalek PE, Li H, Fernandez JM. Prog Biophys Mol Biol 2000;74(1,2):63–91.
[6] Fisher TE, Carrion-Vazquez M, Oberhauser AF, Li H, Marszalek PE, Fernandez JM. Neuron 2000;27(3):435–46.
[7] Fisher TE, Marszalek PE, Fernandez JM. Nat Struct Biol 2000;7(9):719–24.
[8] Best RB, Brockwell DJ, Toca-Herrera JL, Blake AW, Smith DA, Radford SE, et al. Anal Chim Acta 2003;479(1):87–105.
[9] Rounsevell R, Forman JR, Clarke J. Methods 2004;34(1):100–11.
[10] Samori B, Zuccheri G, Baschieri P. Chemphyschem 2005;6(1):29–34.
[11] Oesterhelt F, Oesterhelt D, Pfeiffer M, Engel A, Gaub HE, Muller DJ. Science 2000;288(5463):143–6.
[12] Muller DJ, Baumeister W, Engel A. Proc Natl Acad Sci USA 1999;96(23):13170–4.
[13] Rief M, Gautel M, Oesterhelt F, Fernandez JM, Gaub HE. Science 1997;276(5315):1109–12.
[14] Marszalek PE, Lu H, Li H, Carrion-Vazquez M, Oberhauser AF, Schulten K, et al. Nature 1999;402(6757):100–3.
[15] Carrion-Vazquez M, Oberhauser AF, Fowler SB, Marszalek PE, Broedel SE, Clarke J, et al. Proc Natl Acad Sci USA 1999;96(7):3694–9.
[16] Dietz H, Rief M. Proc Natl Acad Sci USA 2004;101(46):16192–7.
[17] Carl P, Kwok CH, Manderson G, Speicher DW, Discher DE. Proc Natl Acad Sci USA 2001;98(4):1565–70.
[18] Carrion-Vazquez M, Li H, Lu H, Marszalek PE, Oberhauser AF, Fernandez JM. Nat Struct Biol 2003;10(9):738–43.
[19] Brockwell DJ, Paci E, Zinober RC, Beddard GS, Olmsted PD, Smith DA, et al. Nat Struct Biol 2003;10(9):731–7.
[20] Yang G, Cecconi C, Baase WA, Vetter IR, Breyer WA, Haack JA, et al. Proc Natl Acad Sci USA 2000;97(1):139–44.
[21] Chyan CL, Lin FC, Peng H, Yuan JM, Chang CH, Lin SH, et al. Biophys J 2004;87(6):3995–4006.
[22] Li H, Linke WA, Oberhauser AF, Carrion-Vazquez M, Kerkvliet JG, Lu H, et al. Nature 2002;418(6901):998–1002.
[23] Williams PM, Fowler SB, Best RB, Toca-Herrera JL, Scott KA, Steward A, et al. Nature 2003;422(6930):446–9.
[24] Oberhauser AF, Marszalek PE, Erickson HP, Fernandez JM. Nature 1998;393(6681):181–5.
[25] Schwaiger I, Kardinal A, Schleicher M, Noegel AA, Rief M. Nat Struct Mol Biol 2004;11(1):81–5.
[26] Oberhauser AF, Badilla-Fernandez C, Carrion-Vazquez M, Fernandez JM. J Mol Biol 2002;319(2):433–47.
[27] Altmann SM, Grunberg RG, Lenne PF, Ylanne J, Raae A, Herbert K, et al. Structure (Camb) 2002;10(8):1085–96.
[28] Fisher TE, Marszalek PE, Oberhauser AF, Carrion-Vazquez M, Fernandez JM. J Physiol 1999;520(Pt 1):5–14.
[29] Li HB, Oberhauser AF, Fowler SB, Clarke J, Fernandez JM. Proc Natl Acad Sci USA 2000;97(12):6527–31.
[30] Marko JF, Siggia ED. Macromolecules 1995;28(26):8759–70.
[31] Zinober RC, Brockwell DJ, Beddard GS, Blake AW, Olmsted PD, Radford SE, et al. Protein Sci 2002;11(12):2759–65.
[32] Rief M, Fernandez JM, Gaub HE. Phys Rev Lett 1998;81(21):4764–7.

[33] Brockwell DJ, Beddard GS, Paci E, West DK, Olmsted PD, Smith DA, et al. Biophys J 2005;89(1):506–19.
[34] Oberhauser AF, Hansma PK, Carrion-Vazquez M, Fernandez JM. Proc Natl Acad Sci USA 2001;98(2):468–72.
[35] Schlierf M, Li H, Fernandez JM. Proc Natl Acad Sci USA 2004;101(19): 7299–304.
[36] Fernandez JM, Li H. Science 2004;303(5664):1674–8.
[37] Aukhil I, Joshi P, Yan Y, Erickson HP. J Biol Chem 1993;268(4):2542–53.
[38] Jones FS, Jones PL. Dev Dyn 2000;218(2):235–59.
[39] Chiquet M. Matrix Biol 1999;18(5):417–26.
[40] Chiquet-Ehrismann R. Experientia 1995;51(9,10):853–62.
[41] Clark RA, Erickson HP, Springer TA. J Cell Biol 1997;137(3):755–65.
[42] Kannus P, Jozsa L, Jarvinen TA, Jarvinen TL, Kvist M, Natri A, et al. Histochem J 1998;30(11):799–810.
[43] Jarvinen TA, Jozsa L, Kannus P, Jarvinen TL, Hurme T, Kvist M, et al. J Cell Sci 2003;116(Pt 5):857–66.
[44] Rief M, Gautel M, Schemmel A, Gaub HE. Biophys J 1998;75(6): 3008–14.
[45] Florin ELR, M , Lehmann H, Ludwig M, Dornmair C, Moy VT, Gaub HE. Biosens Bioelectron 1995;10:895–901.
[46] Hutter JL, Bechhoefer J. Rev Sci Instrum 1993;64(7):1868–73.
[47] Leahy DJ, Hendrickson WA, Aukhil I, Erickson HP. Science 1992; 258(5084):987–91.
[48] Evans E, Ritchie K. Biophys J 1997;72(4):1541–55.
[49] Izrailev S, Stepaniants S, Balsera M, Oono Y, Schulten K. Biophys J 1997;72(4):1568–81.
[50] Bell GI. Science 1978;200(4342):618–27.
[51] Li H, Carrion-Vazquez M, Oberhauser AF, Marszalek PE, Fernandez JM. Nat Struct Biol 2000;7(12):1117–20.
[52] Clarke J, Hamill SJ, Johnson CM. J Mol Biol 1997;270(5):771–8.
[53] Oberhauser AF, Marszalek PE, Carrion-Vazquez M, Fernandez JM. Nat Struct Biol 1999;6(11):1025–8.